Design of a Photonic Crystal Tapered Coupler with Different Section Lengths Based on Multimode Interference and Mode Matching

2008 Jpn. J. Appl. Phys. 47 1822

(http://iopscience.iop.org/1347-4065/47/3R/1822)

Japanese Journal of Applied Physics
Vol. 47, No. 3, 2008, pp. 1822–1827

Design of a Photonic Crystal Tapered Coupler with Different Section Lengths Based on Multimode Interference and Mode Matching

Ming-Feng LU[1,2*] and Yang-Tung HUANG[2]

[1]*Department of Electronics Engineering, Minghsin University of Science and Technology, No. 1, Hsin Hsin Rd., Hsinfeng, Hsinchu 304, Taiwan*
[2]*Department of Electronics Engineering and Institute of Electronics, National Chiao Tung University, No. 1001, Ta Hsueh Rd., Hsinchu 30010, Taiwan*

(Received August 25, 2007; accepted November 20, 2007; published online March 14, 2008)

Step tapered couplers, which act as mode converters, are usually used between photonic crystal (PC) waveguides and other optical devices for efficient coupling. In this study, the multimode interference (MMI) phenomena in multiple-line-defect PC waveguides are observed. It is found that the optimal length of each section in a PC step tapered coupler is related to the imaging length of MMI. Therefore, a PC step tapered coupler with different section lengths can be designed. Because the modes are matched between two adjacent sections and the scattering losses occurring at the corners of abrupt steps are reduced, it can provide an excellent transmission between PC waveguides and other optical devices. This study also reveals the reason why in some cases, the transmission of PC step tapered couplers decreases counterintuitively when the taper length is increased. [DOI: 10.1143/JJAP.47.1822]

KEYWORDS: coupling, mode matching, multimode interference, photonic crystal, tapered coupler

1. Introduction

Photonic crystals (PCs) are periodic dielectric structures that exhibit photonic band gaps (PBGs) and have attracted extensive interest in recent years. Light propagation with a frequency within the PBGs is forbidden. While line defects are introduced into PCs, the PC waveguides are formed and provide a powerful way to control the flow of electromagnetic waves. To maintain the features of single-mode and PBGs, the core sizes of PC waveguides must be less than one micron. On the contrary, single-mode fibers or other integrated optic devices have sizes on the order of a few microns. Due to the mismatch of core sizes, the coupling losses between PC waveguides and optical fibers that have been verified and reported are on the order of 20–30 dB. Consequently, coupling between PC waveguides and other optical devices becomes a serious problem.

The measurements and further applications of PC devices are also restricted by the coupling issues. Thus, there have been many couplers proposed for efficient transmission. Compact mode converters with low coupling loss, including gratings,[1–4] lens or mirrors,[5,6] and tapered structures[7–9] are now becoming key building blocks in integrated PC systems. The tapered coupler is the most popular device in connecting PC waveguides with other optical devices. The waveguide taper was used for efficient light coupling between dielectric and PC waveguides.[10] As a result of resonant tunneling in an adiabatic coupling, the transmission coefficient of a tapered slab waveguide at resonant frequencies was high.[11] A mathematical model derived from the step theory was proposed to calculate the transmission efficiency of waveguide tapers.[12] A slow and continuous transition is required in conventional taper structures; thus, these types of couplers are very long.[13] On the other hand, the size of a PC tapered coupler can be much smaller than that of a conventional waveguide taper due to its large dispersion of modes. Various designs for segmented PC tapers were compared and it was found that in some cases the transmission decreases counterintuitively when the taper length is increased.[14] Mode matching techniques for highly efficient coupling based on setting localized defects in PC tapered waveguides were studied.[15–18] Furthermore, PC continuous tapers were designed by varying progressively the radii of air holes for low-loss direct coupling.[19–21]

The highest transmission efficiency of those coupling structures can be greater than 90%. However, the optimal design methodologies of PC tapered couplers are not clear till now. Note that the section lengths in a conventional PC step tapered coupler are the same. To find out what the optimum length of each section in a PC step tapered coupler is and why the transmission decreases counterintuitively when the taper length is increased in some cases, we inspect the multimode interference (MMI) phenomena in multiple-line-defect PC waveguides.

The MMI phenomenon is an observable fact in multimode devices. On the basis of the self-imaging principle, a field profile can be reproduced in single or multiple images at regular intervals along the path of propagation.[22] The MMI effect can be introduced in optical power splitters/combiners, switches, Mach–Zehnder interferometers, and other applications. However, in the field of PCs, only a few researchers focus on this topic. Power splitters based on the MMI effect in PC waveguides have been presented.[23,24] Wavelength demultiplexers can be realized by the combination of MMI and PCs.[25–27]

In this study, the design of a PC tapered coupler with different section lengths based on the MMI effect and mode matching is proposed. We find out that the optimal length of each section in a PC step tapered coupler is related to the imaging length of MMI. The mode profiles between two adjacent sections are matched in the well-designed taper coupler and the scattering losses occurring at the corners of abrupt steps can be eliminated. It provides excellent coupling between PC waveguides and other optical devices. This study also reveals why in some cases the transmission of PC step tapered couplers decreases counterintuitively when the taper length is increased.

*E-mail address: mflu@must.edu.tw

In the real world, a taper structure is a three-dimensional (3D) problem. The finite heights and radiation losses are issues that need to be taken into account in practical 3D PC devices. However, we can investigate the MMI phenomena and find out the physics easily in a simplified two-dimensional (2D) model. While a 3D problem is converted to a 2D model, the dielectric constant of the host medium must be replaced by its effective index. In the following sections, the MMI phenomena in 2D PC waveguides will be discussed. The design method of a PC tapered coupler with different section lengths based on the MMI effect and mode matching will be presented. Finally, the validity and robustness of our method will be proven by two test cases.

2. MMI in PC Waveguides

To explore the transmission mechanism behind PC tapered couplers, first we investigate the MMI in the PC structure that was utilized in ref. 14 as shown in Fig. 1. The PC tapered coupler connects one input ridge waveguide and one output single-line-defect PC waveguide. In this structure, the material of the matrix is GaAs/$Al_{0.6}Ga_{0.4}As$. The effective indices of the ridge waveguide and the cladding layer are 3.343 and 3.342, respectively; therefore, the wave within the 1.6-μm-wide ridge waveguide is weakly guided. The PC structure is a triangular lattice of air holes with a lattice constant $a = 0.25\,\mu m$ and an air hole radius $r = 0.3a$, which results in a transverse-electric (TE) bandgap only in the frequency range from 0.211 to 0.282 (a/λ). TE polarization indicates that the electric field is perpendicular to the normal of the lattice plane, which follows the convention used in a photonic crystal. The single-line-defect PC waveguide is formed by removing one row of air holes along the Γ–K direction in the triangular lattice and denoted by a W1 PC waveguide. Wn stands for a PC waveguide with n rows of air holes removed. Consequently, the PC tapered coupler is composed of W3, W5, and W7 sections. A Gaussian wave with a wavelength λ of 1 μm is launched from the ridge waveguide to test the transmission efficiency of the PC tapered coupler.

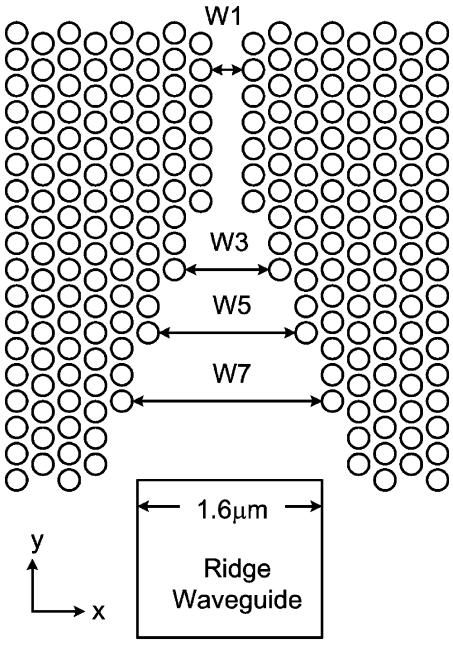

Fig. 1. The PC step tapered coupler connects one input ridge waveguide and one output single-line-defect PC waveguide. The PC structure is a triangular lattice of air holes with a lattice constant $a = 0.25\,\mu m$ and an air hole radius $r = 0.3a$. The effective indices of the ridge waveguide and the cladding layer are 3.343 and 3.342, respectively.

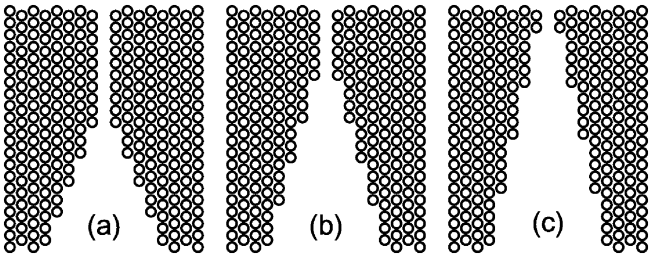

Fig. 2. Various lengths of PC tapered couplers used to compare their transmission from a 1.6-μm-wide ridge waveguide to a single-line-defect PC waveguide. The section lengths of each segment in the PC tapered coupler are 2.5a, 3.5a, and 4.5a in cases (a), (b), and (c), respectively.

Various lengths of PC tapers shown in Fig. 2 are used to compare their transmission abilities from a 1.6-μm-wide ridge waveguide to a single-line-defect PC waveguide. The transmission is calculated by the 2D finite-difference time-domain (FDTD) method. The spatial and temporal grid sizes used in the FDTD method are $a/16$ and $a/64$, respectively. These meet the requirements of the Courant condition;[28] thus, convergent and stable results can be obtained. Perfectly matched layers are applied to the four sides of the computational domain to delimit the boundary. In case (a), the step size in length is two lattices; therefore, the section length of this PC tapered coupler is equivalent to 2.5a. The transmission through this tapered coupler is 68.9%. For case (b), the section length of each segment is 3.5a, and its transmission increases to 79.8%. While in case (c), the length of each section is extended to 4.5a, but its transmission drops to 55.7%. The transmission decreases counterintuitively when the taper length is increased. These data can also be found from the curves in Fig. 2 of ref. 14.

First we observe the MMI phenomena in multiple-line-defect PC waveguides to reveal the relation between the optimized section length of a tapered coupler and the imaging length of MMI. In Figs. 3(a) and 3(b), a Gaussian light source with a width equal to the waveguide width of W1 is launched from W1 to W3 or from W3 to W1, respectively. It is obvious that self-imaging exists in W3 PC waveguides in both cases. The dual-head arrows in these figures represent the distances between two single images and they come into view at regular intervals with a period equal to 8a. The first two-fold image appears at 4a, which is a half of the single-image distance.

Next, we show that the transmission between two PC waveguides with different widths is related to the section length of the PC waveguide. In Fig. 4, a Gaussian wave with wavelength $\lambda = 1\,\mu m$ propagates from the wider to the narrower PC waveguide. The initial position of the light source located within the wider waveguide is arbitrarily selected away from the interface between two waveguides and then moved toward the interface. The transmission efficiency from the wider to the narrower PC waveguide varies periodically with the position of the light source as shown in Fig. 4. In other words, the transmission is related

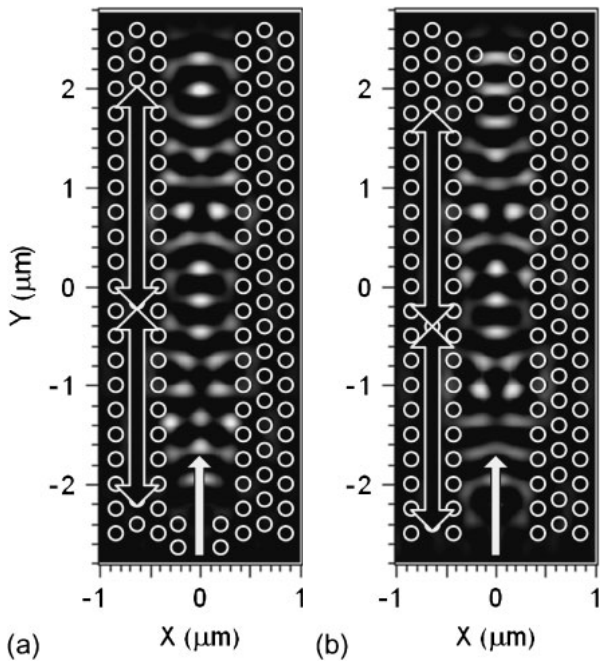

Fig. 3. Self-imaging phenomena in multiple-line-defect PC waveguides. The light is launched (a) from W1 to W3, and (b) from W3 to W1. The dual-head arrows represent the distances between two single images.

to the section length of the input waveguide. In case (a), the transmission efficiency from the W3 to the W1 PC waveguide is between 0.65 and 0.86, and its magnitude oscillates in a period of about 8*a*. In cases (b) and (c), the transmission efficiencies from W5 to W3 and from W7 to W5 are 0.87–0.94 and 0.90–0.94, respectively. The oscillation period is about 1*a* for both cases. Obviously, there are a larger variation of transmission efficiency and a longer oscillation period in case (a); thus, the section length of W3 in a PC step tapered coupler must be well designed.

The number of modes in a waveguide and the dissimilarity of mode profiles between waveguides affect the efficiency of power conversion. Most of the power loss occurs at the interface of two sections due to the spatial mismatch of waveguides. It has been found that the scattering loss happened mainly at the corners of the abrupt steps.[13,21] As the waveguide width decreases, so does the number of modes in the waveguide. Since the number of available modes into the PC waveguide falls, the transmission efficiency decreases as well.[10] The W1 waveguide has the fewest modes that can be excited and the narrowest width, which lowers the efficiency of power conversion from W3 to W1.

However, the transmission efficiency between two PC waveguides with different widths can be high if the light source is placed at the positions with transmission peaks according to the results in Fig. 4. That is equivalent to tuning the section length of the wider waveguide. In Fig. 4(a), the magnitude of transmission efficiency from W3 to W1 oscillates with a period of about 8*a*, which is the same as the single-image distance of MMI in the W3 waveguides shown in Fig. 3. We may conclude that the optimal length of each segment in a PC step tapered coupler is related to the imaging length of MMI. This concept will be evident in the discussion in next section.

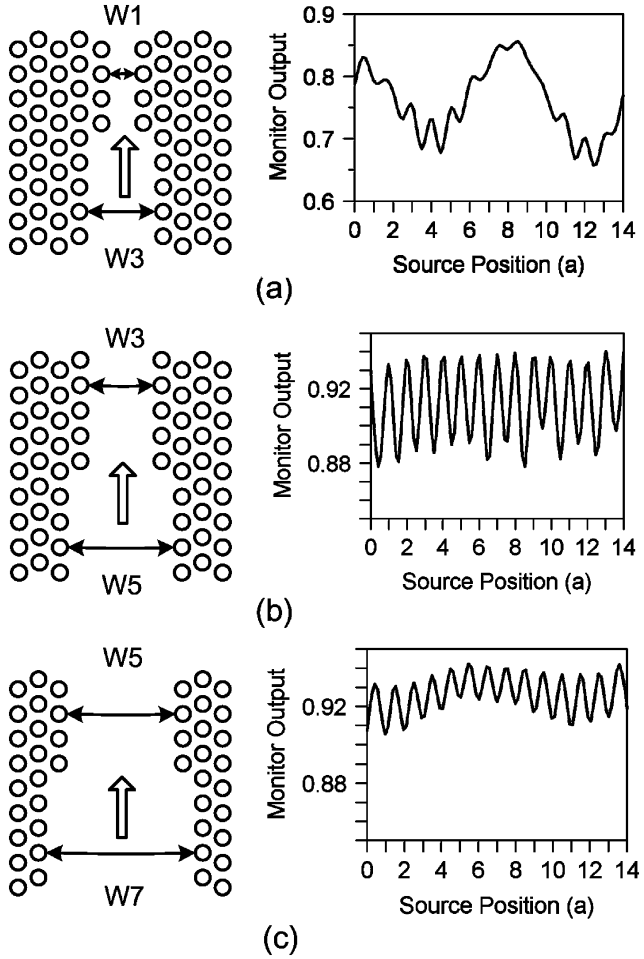

Fig. 4. A Gaussian wave is launched from the wider to the narrower section to test the transmission between two PC waveguides with different widths. The transmission efficiencies (a) from W3 to W1, (b) from W5 to W3, and (c) from W7 to W5 vary periodically with the launch position of the light source.

3. Design of a PC Tapered Coupler with Different Section Lengths Based on Multimode Interference and Mode Matching

As discussed before, the major transmission loss occurs due to the mismatch of mode images between the contiguous sections and the section length of W3 in a PC tapered coupler is the key parameter to be determined. Let us examine the mode profile in each section. Figure 5(a) shows the projected band diagram of the single-line-defect PC waveguide calculated by the plane wave expansion (PWE) method. The gray regions in the band diagram are zones where PC guided modes exist.[29] Those below the first gray region are index guiding modes, and they fold back into the first Brillouin zone at the zone boundary. The white region between two gray zones is the photonic bandgap. For line-defect PC waveguides, PC guiding modes exist in the PBG. The field profile of the fundamental defect mode in the W1 PC waveguide shown in Fig. 5(b) is obviously an even mode.

Figure 5(c) shows the projected band diagram of the W3 PC waveguide. Modes e3, e4, and e5 situated in the bandgap are PBG guiding modes. These modes in the wide defect region of the waveguide lead to the operation of MMI. The

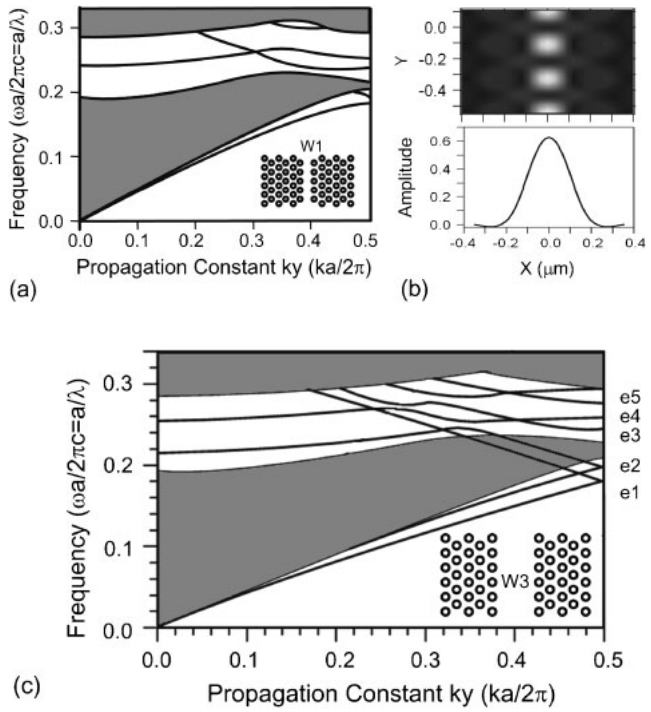

Fig. 5. (a) Projected band diagram of the single-line-defect PC waveguide. (b) Field profile of the fundamental mode in the W1 PC waveguide. (c) Projected band diagram of the W3 PC waveguide.

working frequency a/λ is equal to 0.25 and it can be seen that there are three modes at that frequency. The propagation constants of the fundamental and second-order modes are 0.42 and 0.28, respectively. The single-image distance of MMI is approximately $2\pi/(k_0 - k_2) = 7.14a$, where k_0 and k_2 are the wave numbers of these two modes.[23] Because the PWE method can not be used to treat problems with loss and dispersion, it should be emphasized that the results evaluated from this band diagram have a large deviation. By using the FDTD method, the distance between two single images can be precisely obtained and is equal to $7.8a$. The first two-fold image appears at $3.9a$.

If the section length of W3 is adjusted to $3.9a$, the wave can be coupled smoothly from the W3 to the W1 PC waveguide by mode matching. The section length of W3 in a PC step tapered coupler can be fine-tuned from $3.5a$ to $3.9a$ by adjusting the positions of the first two air holes of the W1 waveguide as shown in Fig. 6. Therefore, a PC step tapered coupler with different section lengths can be constructed. We choose the taper structure in Fig. 2(a), and the section length of W3 is fine-tuned from $2.5a$ to $3.9a$. The MMI phenomenon in the well-designed PC tapered coupler is shown in Fig. 7(a). Whereas the section length of W3 is changed from $2.5a$ to $3.9a$, the transmission efficiency of this tapered coupler is markedly improved from 68.9 to 87.4%. The improvement is mainly due to the mode matching between the W3 and W1 PC waveguides. The transmission is 83.1% when the section length of W3 is $3.5a$, and it drops to 73.5% when the section length of W3 is extended to $4.5a$. The power profiles in the W1 PC waveguide and at the entrance of the W3 section are shown in Figs. 7(b) and 7(c), respectively. The wave of a two-fold image at the entrance of the W3 section can couple smoothly

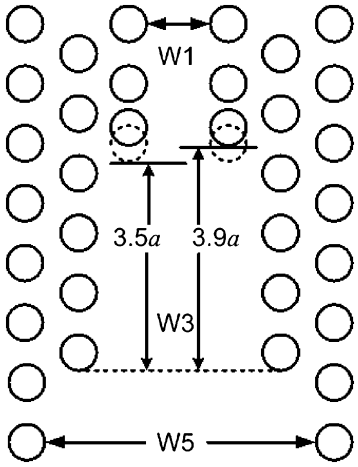

Fig. 6. The section length of W3 in a PC step tapered coupler can be fine-tuned from $3.5a$ to $3.9a$ by adjusting the positions of the first two air holes of the W1 waveguide.

into the W1 PC waveguide, which supports the single mode only through one two-fold-image distance. While the section length of W3 is elongated out of the range of two-fold-image distance, the modes are no longer well matched and the wave will not be coupled smoothly from the W3 to the W1 PC waveguide. The mode conversion is reduced when the section length of a PC step tapered coupler is out of the imaging length of MMI. Therefore, the transmission of a PC step tapered coupler varies periodically with the section lengths. This explains why the transmission decreases counterintuitively in some cases when the taper length is increased. The transmission of a PC step tapered coupler does not increase as the taper length increases, which is different from the case of a conventional waveguide taper. In a conventional waveguide taper, a long taper length is required for an adiabatic mode conversion. The transmission spectrum as a function of the operating wavelength of the well-designed PC tapered coupler is shown in Fig. 7(d). It can be seen that the device has a broadband transmission characteristic. Compared with those structures in which high transmissions are achieved using interface resonant modes, whose bandwidths are limited by the resonance width,[10] in our design the PC tapered coupler with different section lengths gives a nonresonant way of coupling; the device can have a wider frequency range for high transmission.

The validity and robustness of our method are demonstrated by two test cases. The structure of the first test case shown in Fig. 8 is the same as that of the case in Fig. 2(a) except that the section length of W3 in the PC tapered coupler is adjusted from $2.5a$ to $11.7a$, which is the length of one two-fold-image distance plus one single-image distance. The transmission efficiency of this tapered coupler is improved from 68.9 to 82.9%, which is slightly smaller than the best one in Fig. 7(a) but is still greater than the nonoptimized case. Transmission improvement by introducing the concept of the imaging length of MMI to design a PC tapered coupler was affirmed by this test case.

Coupling efficiencies can also be improved by changing the radii of air holes in PC couplers, but the corresponding design methodologies are difficult to perform.[30,31] In the

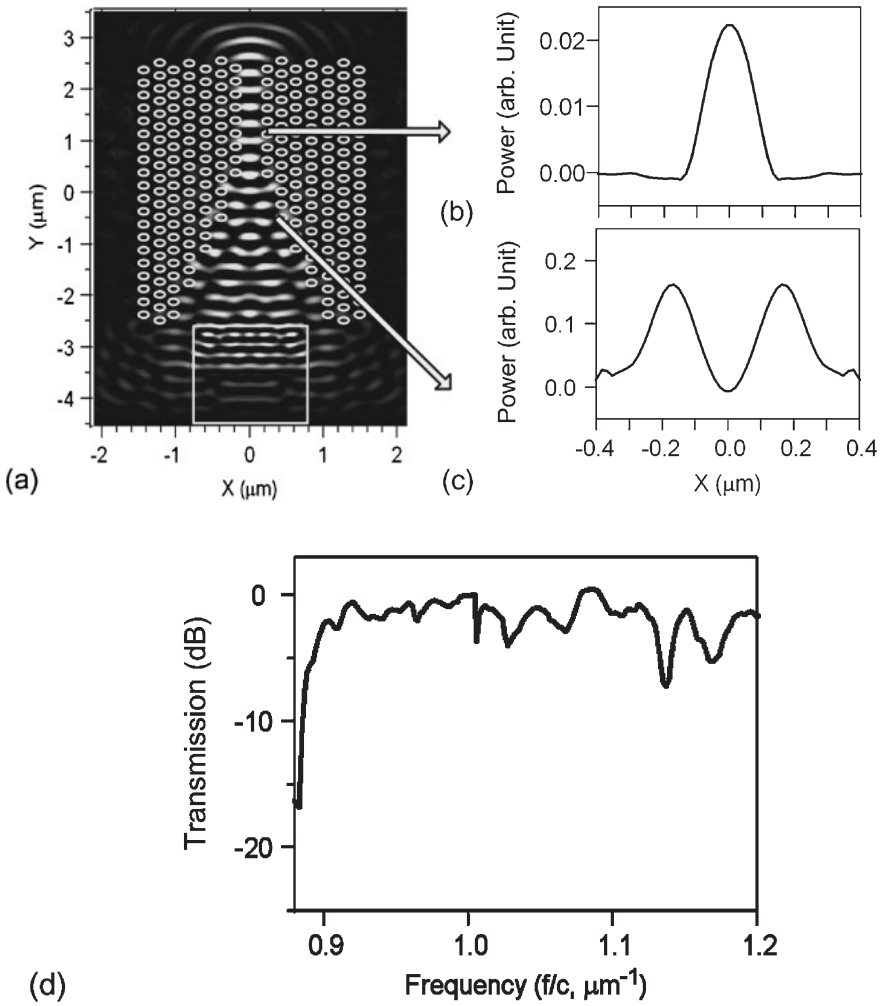

Fig. 7. (a) MMI phenomenon in the well-designed PC tapered coupler with different section lengths. The taper structure is the same as the case in Fig. 2(a) except that the section length of W3 is fine-tuned from 2.5*a* to 3.9*a*. (b) Power profile of a single image in the W1 PC waveguide. (c) Power profile of two-fold image at the entrance of the W3 PC waveguide. (d) Transmission spectrum of the well-designed PC tapered coupler as a function of the operating wavelength.

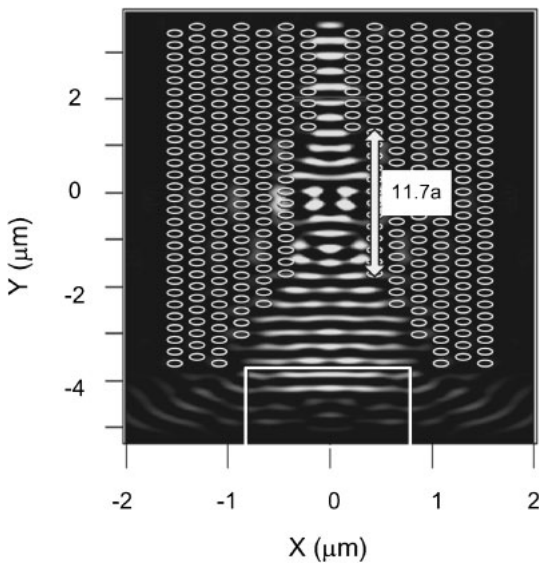

Fig. 8. The taper structure of the first test case is the same as that of the case in Fig. 2(a) except that the section length of W3 is adjusted from 2.5*a* to 11.7*a*, which is the length of one two-fold-image distance plus one single-image distance.

second test case, the correlation between the radii of air holes and the coupling efficiency of tapered couplers will be discussed. The structure of the second test case is the same as that of the case in Fig. 2(a) except that the section length of W3 is 3.5*a*. As shown in Fig. 9(a), the original radius of the first two air holes of the W1 waveguide is 0.3*a* (the dashed line circles) and we regulate it to see the variation of transmission. The transmission of the PC tapered coupler as a function of the radius of the first two air holes of the W1 waveguide is shown in Fig. 9(b). When the radius of the modified air holes is reduced to 0.16*a* (the solid line circles), the transmission reaches its maximum, i.e., 85.1%. The efficiency improvement is partially from the expansion of the waveguide width. However, note that the section length of W3 after fine tuning is equivalent to 3.84*a*, which is almost the same as the single-image distance of MMI, i.e., 3.9*a*. Altering the radius of the first two air holes in the W1 waveguide is equivalent to modifying the section length of W3. As a result of mode matching between the two neighboring sections, the transmission of this PC tapered coupler can be improved. This explains why we can achieve high coupling efficiency by adjusting the radii of air holes in PC segmented taper couplers.

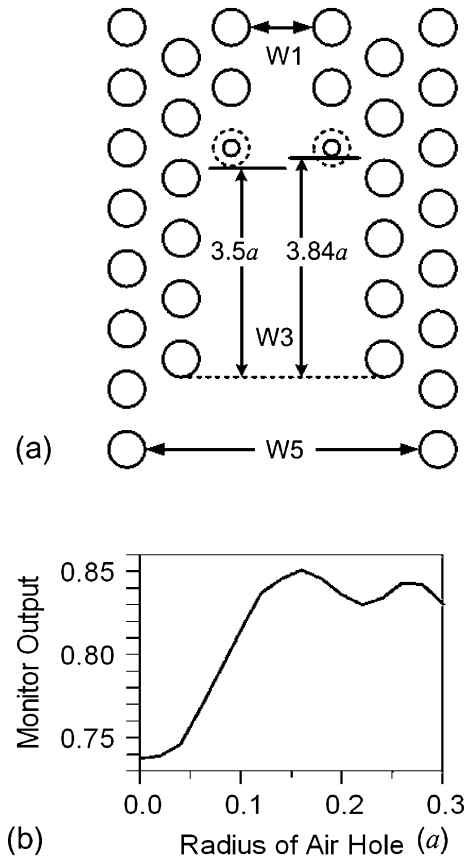

Fig. 9. (a) The taper structure of the second test case is the same as that of the case in Fig. 2(a) except that the section length of W3 is 3.5a. The radius of the first two air holes of the W1 waveguide is modified from 0.3a (the dashed line circles) to 0.16a (the solid line circles). The equivalent section length of W3 after fine tuning is 3.84a. (b) Transmission as a function of the radius of the first two air holes of the W1 waveguide. The maximum coupling efficiency is 85.1% when the radius of the modified air holes is 0.16a.

4. Conclusions

PC devices with taper structures can be easily coupled with other optical elements, such as single-mode optical fibers, slab waveguides, and ridge waveguides. In conventional PC step tapered couplers, the length of each segment is the same and their transmission efficiencies are inhibited. Some researchers concluded that the PC tapers have to be lengthened to increase their coupling ability. In this study, it is found that the section length in a PC tapered coupler plays a crucial role and is related to the imaging length of MMI. Therefore, a PC step tapered coupler with different section lengths can be designed on the basis of multimode interference. The optimal structure can provide mode matching between two adjacent sections and reduce the scattering loss occurring at the corners of abrupt steps. In the case we studied, when the section length of W3 is fine-tuned from 2.5a to 3.9a, the transmission efficiency of this tapered coupler is improved significantly from 68.9 to 87.4%. Thus, the PC step tapered coupler with different section lengths designed on the basis of MMI can provide high transmission efficiency between PC waveguides and other optical devices.

Acknowledgment

This work was supported in part by the National Science Council of the Republic of China under grants NSC 95-2221-E-159-015.

1) T. Liang and R. W. Ziolkowski: IEEE Photonics Technol. Lett. **10** (1998) 693.
2) R. W. Ziolkowski and T. Liang: Opt. Lett. **22** (1997) 1033.
3) D. Taillaert, W. Bogaerts, P. Bienstman, T. F. Krauss, P. V. Daele, I. Moerman, S. Verstuyft, K. D. Mesel, and R. Baets: IEEE J. Quantum Electron. **38** (2002) 949.
4) W. Kuang, C. Kim, A. Stapleton, and J. D. O'Brien: Opt. Lett. **27** (2002) 1604.
5) M. Potter and R. Ziolkowski: Opt. Express **10** (2002) 691.
6) D. W. Prather, J. Murakowski, S. Shi, S. Venkataraman, A. Sharkawy, C. Chen, and D. Pustai: Opt. Lett. **27** (2002) 1601.
7) P. E. Barclay, K. Srinivasan, and O. Painter: J. Opt. Soc. Am. B **20** (2003) 2274.
8) M. Notomi, A. Shinya, S. Mitsugi, E. Kuramochi, and H. Y. Ryu: Opt. Express **12** (2004) 1551.
9) M. Palamaru and Ph. Lalanne: Appl. Phys. Lett. **78** (2001) 1466.
10) A. Mekis and J. D. Joannopoulos: J. Lightwave Technol. **19** (2001) 861.
11) Y. Xu, R. K. Lee, and A. Yariv: Opt. Lett. **25** (2000) 755.
12) E. H. Khoo, A. Q. Liu, J. H. Wu, J. Li, and D. Pinjala: Opt. Express **14** (2006) 6035.
13) R. S. Balmer, J. M. Heaton, J. O. Maclean, S. G. Ayling, J. P. Newey, M. Houlton, P. D. J. Calcott, D. R. Wight, and T. Martin: J. Lightwave Technol. **21** (2003) 211.
14) T. D. Happ, M. Kamp, and A. Forchel: Opt. Lett. **26** (2001) 1102.
15) P. Sanchis, J. Marti, J. Blasco, A. Martinez, and A. Garcia: Opt. Express **10** (2002) 1391.
16) C. W. Chang, S. C. Cheng, and W. F. Hsieh: Opt. Commun. **242** (2004) 517.
17) J. Jiang, J. Cai, G. P. Nordin, and L. Li: Opt. Lett. **28** (2003) 2381.
18) Y. F. Chau, T. J. Yang, and W. D. Lee: Appl. Opt. **43** (2004) 6656.
19) P. Pottier, I. Ntakis, and R. M. De La Rue: Opt. Commun. **223** (2003) 339.
20) A. Xing, M. Davanço, D. J. Blumenthal, and E. L. Hu: IEEE Photonics Technol. Lett. **17** (2005) 2092.
21) A. Talneau, Ph. Lalanne, M. Agio, and C. M. Soukoulis: Opt. Lett. **27** (2002) 1522.
22) L. B. Soldano and E. C. M. Pennings: J. Lightwave Technol. **13** (1995) 615.
23) T. Liu, A. R. Zakharian, M. Fallahi, J. V. Moloney, and M. Mansuripur: J. Lightwave Technol. **22** (2004) 2842.
24) C.-C. Lin and S.-L. Tsao: Proc. SPIE **5907** (2005) 59070W.
25) H. J. Kim, Insu Park, B. H. O, S. G. Park, E. H. Lee, and S. G. Lee: Opt. Express **12** (2004) 5625.
26) T. Y. Tsai, Z. C. Lee, J. R. Chen, C. C. Chen, Y. C. Fang, and M. H. Cha: IEEE J. Quantum Electron. **41** (2005) 741.
27) L. W. Chung and S. L. Lee: Opt. Express **14** (2006) 4923.
28) R. Courant, K. Friedrichs, and H. Lewy: IBM J. Res. Dev. **11** (1967) 215.
29) M. Loncar, T. Doll, J. Vuckovic, and A. Scherer: J. Lightwave Technol. **18** (2000) 1402.
30) P. Lalanne and A. Talneau: Opt. Express **10** (2002) 354.
31) G. Chietera, A. H. Bouk, F. Poletti, F. Poli, S. Selleri, and A. Cucinotta: Microwave Opt. Technol. Lett. **42** (2004) 196.